Analysis of the structural performance of reinforced concrete under fire loading

Dilshod Imamaliev[1], Amirkhan Sazairov[2], Reyhan Akbarli[3]
[1]Department of Construction and Maintenance of Automobile Roads, Tashkent State Transport University, Tashkent, Uzbekistan
[2, 3]Department of Mechanics, Azerbaijan University of Architecture and Construction, Baku, Azerbaijan
[1]Corresponding author
E-mail: [1]*dilimshod@gmail.com*, [2]*sazairov_emirxan@mail.ru*, [3]*reyhan.akbarli@azmiu.edu.az*

Received 27 October 2025; accepted 18 November 2025; published online 22 December 2025
DOI https://doi.org/10.21595/vp.2025.25762

Check for updates

74th International Conference on Vibroengineering in Tashkent, Uzbekistan, November 27-29, 2025

Abstract. This study examined the behavior of reinforced concrete structures when exposed to high temperatures resulting from fire. Deterioration in material strength due to fire exposure alters a reinforced concrete structure's load-bearing capacity and overall behavior. Elevated temperatures negatively affect key material properties of reinforced concrete, including density, coefficient of thermal expansion, thermal conductivity, and elastic modulus. As a result, if a structure experiences fire either concurrently with or prior to an earthquake, these changes in material properties will significantly influence its dynamic performance. For the numerical simulation, the selected structure was designed with a formwork plan and load-bearing system in accordance with earthquake-resistant design principles. Based on this design, fixed and variable loads acting on the beams were assigned. By promoting resilient infrastructure capable of withstanding severe environmental conditions such as earthquakes and fires, this study contributes to the achievement of sustainable development goals. It underscores the necessity of integrating fire resistance into earthquake-resistant design to foster disaster-resilient urban development. The findings may encourage more flexible and sustainable construction practices aligned with SDGs 9 (Industry, Innovation and Infrastructure), 11 (Sustainable Cities and Communities), and 13 (Climate Action).

Keywords: high temperatures, concrete reinforcement, load-bearing capacity, coefficient of thermal expansion, temperature-dependent variations, resilient urban development, sustainable infrastructure, earthquake engineering, fire resistance, effects of climate change on structures.

1. Introduction

Many countries have reinforced their fire-safety regulations following major fires and conflicts. For instance, Italy has intensified its regulatory framework, and the Regulation on Fire Protection of Buildings now establishes key architectural requirements in addition to provisions for detection and suppression systems. Recent studies further reflect this shift: [13] investigates the impact of fire cut-offs on airflow within ventilated facade cavities, providing engineering assessments of solid and perforated cut-offs in Azerbaijan and underlining the need for updated design solutions. Other research [6,14] employs ANSYS finite element modelling to evaluate the flexural response and ductility of reinforced concrete beams with GFRP reinforcement, demonstrating that higher GFRP ratios improve load-carrying performance.

Post-earthquake fire (PEF) effects on buildings are examined in several studies [1-4], which emphasize that fire loads applied after seismic and gravity actions significantly reduce the residual capacity of damaged structures, highlighting the need for further investigation in seismically active regions. Additional findings in [7] confirm that sequential fire loading further weakens already compromised elements. Recent work also demonstrates the potential of data-driven approaches: for example, machine-learning models have been successfully used to predict the properties of aerated concrete incorporating ash–slag waste [15], offering new opportunities for performance assessment in environments prone to both seismic and fire hazards.

Further studies [16–19,20] investigate advanced reinforcement strategies and the elastoplastic behavior of structural elements under complex loading, incorporating hardening, softening and damage evolution-factors essential for understanding the interaction between seismic and fire effects. Research on temperature-induced structural transitions [21] likewise clarifies how thermal exposure alters material properties, providing important insights for fire-affected infrastructure. Recent material innovations also contribute to improved fire resistance and structural performance: 3D-printed LC3-based engineered cementitious composites [22, 23] show enhanced beam behavior, mechanical properties and controlled anisotropy, demonstrating promising approaches for developing more resilient and energy-efficient structural systems.

2. Fire curves

Fire temperatures over time are commonly estimated using zone models, room-fire models and standard fire curves. Among these, ASTM E119 and ISO 834 are the most widely applied, representing the standard forms of the natural and experimental curves described by Buchanan (2001). These models assume a uniform gas temperature within the compartment and do not account for flame spread or smoke movement, making them most suitable for post-flashover conditions. The ISO 834 temperature-time relationship used to define high-temperature degradation of concrete properties is expressed by Eq. (1):

$$T = T_0 + 345\log(8t+1). \tag{1}$$

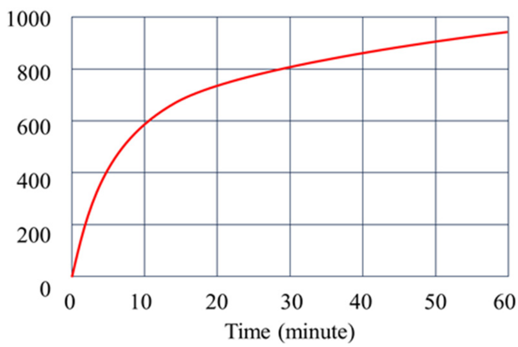

Fig. 1. Temperature variation over time in relation to the duration of the fire

Understanding fire-induced temperature development and the resulting degradation of material properties is essential for evaluating structural performance at high temperatures. Although concrete is non-combustible, its mechanical and physical characteristics deteriorate as temperature increases. This degradation becomes particularly pronounced above 600 °C, at which point concrete may lose nearly half of its strength – a level commonly referred to as the critical temperature [8-10].

This study advances the field in three key aspects. First, it introduces a temperature-dependent modelling framework for reinforced concrete frames subjected to ISO 834 fire, directly linking material degradation in SAP2000 to global seismic response indicators. Second, it quantifies the combined influence of elevated temperature and seismic loading on lateral displacements, base shear and internal forces, and evaluates the resulting drift demands against typical code-based limits for RC structures. Third, it provides practical guidance by identifying temperature ranges in which seismic performance remains within acceptable drift limits, while safety margins notably diminish, thereby indicating when second-order effects and soft-storey behaviour may become critical in fire-affected RC frames.

ISSN PRINT 2345-0533, ISSN ONLINE 2538-8479

3. Material and method

We'll look at a building meant for residential use. The structure has four stories, three x-directional spans, two y-directional spans, and three spacing between them. The SAP2000 software will be used to model and analyze the structure. C30/37 is the concrete class selected for the design.

Table 1. Gives general details about the planned structure

Property	Value
Building use purpose	Residential
Number of Floors	Ground + 3 Floors
Floor height	3 m
Flooring	Ribbed Slab
Foundation	Continuous Foundation
Concrete class	C30/C37
Steel class	B420C
Beam dimensions	b_w = 25 cm, h = 40 cm
Column dimensions	b = 30 cm, h = 60 cm
	b = 60 cm, h = 30 cm
Soil class	ZB (Slightly weathered, moderately strong rocks)
Building use class	3
Building importance factor (I)	1
Concrete elastic modulus (E)	32000 MPa
Live loads (q)	In Rooms: 2 kN/m^2
	On Stairs: 3.5 kN/m^2
	On Balconies: 5 kN/m^2

A formwork plan was developed in accordance with earthquake-resistant design principles, and the architectural layout was prepared within the scope of the study. Preliminary sizing of structural elements followed the relevant standards and regulations. The structural system was then modelled in SAP2000 using the selected section dimensions, calculated beam loads and defined material properties. Seismic analysis was performed in SAP2000 using the Modal Combination Method [11, 12].

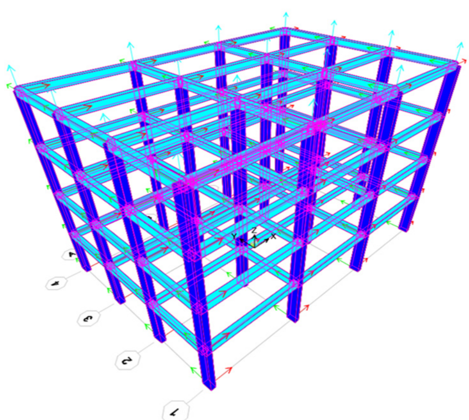

Fig. 2. Model of the modeled structure created in Sap2000

For each floor level, the dynamic analysis uses three dynamic degrees of freedom, which represent rotational motion around the z-axis and translational motion in the x and y directions. Consequently, each floor level has a total of three degrees of freedom. A four-story building has twelve dynamic degrees of freedom in total. Therefore, there should be twelve mode shapes in the structure. The table contains the periods and additional details about the modes gleaned from the modal analysis.

Table 2. The building's natural vibration frequencies and periods

Modal periods and frequencies	Eigenvalue (rad^2/sn^2)	Period (s)	Frequency (Hz)
1	0.932045	1.07291	0.932045
2	0.815862	1.22569	0.815862
3	0.752464	1.32897	0.752464
4	0.263753	3.79143	0.263753
5	0.232894	4.29379	0.232894
6	0.216319	4.62281	0.216319
7	0.127348	7.85249	0.127348
8	0.112993	8.85008	0.112993
9	0.105233	9.50271	0.105233
10	0.081042	12.33924	0.081042
11	0.07197	13.89459	0.07197
12	0.066917	14.94389	0.066917

Temperature Assignment to the Structure: When evaluating reinforced concrete structural elements exposed to high temperatures (fire), it is essential to account for the temperature-dependent degradation of material properties. In this study, a standard compartment fire was represented by the ISO 834 fire curve. The fire was assumed to affect only the structural elements at the ground floor, where the columns are critical for the global stability of the frame, while the upper-story elements remained at ambient temperature (20 °C).

In SAP2000, the fire scenario was modeled by assigning temperature-dependent concrete properties to the ground-floor columns at discrete temperature levels (20-680 °C). For each level, the corresponding reductions in Young's modulus and density from Table 3 were applied only to the heated columns, while all other elements retained their original properties. Each analysis case therefore represents the same gravity and seismic loading, but with progressively reduced stiffness and mass in the fire-exposed columns. This procedure provides a direct and consistent link between the temperature-dependent material data in Table 3 and the displacements and internal forces presented in the Results section.

Table 3. Temperature-dependent material properties of concrete used in the analysis for the fire-exposed ground-floor columns

Time (min)	Temperature (°C)	Young's modulus (E) (MPa)	Density (ρ) (kg/m^3)
0	20	32000	2500
1	349	22450	2394
2	445	16352	2365
3	502	12653	2353
4	544	9991	2344
5	576	7910	2336
6	603	6200	2331
7	626	4750	2326
8	645	3491	2321
12	705	0	2308
20	781	0	2292
30	842	0	2278
40	885	0	2269
50	918	0	2262
60	945	0	2256

The values of Young's modulus and density at each temperature were used directly in the SAP2000 model for the fire-exposed ground-floor columns. Other thermal parameters (such as specific heat and thermal conductivity) were not required in the structural analysis and are therefore not listed here.

All figures in this paper are original and were prepared by the authors based on their own numerical simulations in SAP2000.

4. Results

The mass and elastic modulus of the material decrease with increasing temperature, resulting in an increase in the structure's first periods in both the x and y directions. Up to 300 °C, this increase is slight, but after that, it has greatly increased, especially at 600 °C, when it is roughly twice as high as it was at the beginning.

Table 4. Joint’s displacements based on temperature (mm)

Node	20 °C	100 °C	200 °C	300 °C	400 °C	500 °C	600 °C	680 °C
1	0.56	0.56	0.55	0.61	0.70	0.86	1.21	2.70
2	1.48	1.49	1.47	1.62	1.86	2.26	3.19	7.08
3	2.31	2.31	2.29	2.52	2.89	3.52	4.95	11.00
4	2.92	2.92	2.89	3.18	3.65	4.44	6.25	13.89

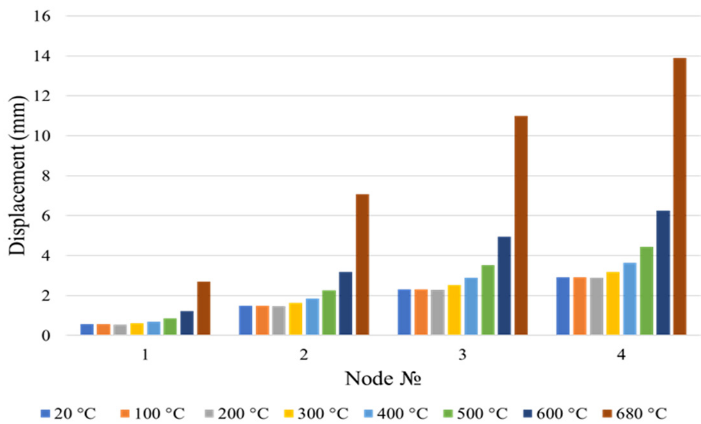

Fig. 3. Joint displacements as a function of temperature (mm)

Modal effective masses have decreased as a result of rising temperatures and longer structure periods, which has decreased the structure’s base shear forces. Although this decline is not very noticeable until 300 °C, it has since accelerated, especially reaching about 46 % at 600 °C.

Table 5. Base shear force

Temperature (°C)	V_{tx} (kN)	V_{ty} (kN)
20	58	66
100	58	66
200	57	65
300	51	59
400	45	52
500	36	43
600	27	31

The reduction in lateral stiffness leads to increased nodal displacements, even though base shear decreases with temperature. This increase is modest up to 300 °C but becomes more pronounced at higher temperatures, reaching about 2.16 times the initial displacement at 600 °C (Table 4). At 680 °C, the maximum roof-node displacement is 13.89 mm compared to 2.92 mm at 20 °C. For the 12 m building height, this corresponds to a drift ratio of approximately 0.12 %, which remains well below typical code limits of 1-2 % for RC structures. Thus, within the examined temperature range, the rise in displacements does not exceed standard serviceability or ultimate drift thresholds, although it noticeably reduces the structural safety margin.

Seismic floor forces decrease due to the reduction in base shear under earthquake loading. With increasing temperature, axial forces, shear forces and bending moments in columns and beams also decline; at 600 °C the internal forces remain about 93 % of those at 20 °C, indicating that the load-bearing capacity is not fully exhausted, consistent with previous observations for fire-exposed RC columns [5]. However, the combined effect of larger lateral displacements and reduced stiffness shows that the structure is approaching conditions where second-order effects and soft-storey behaviour may become critical if temperatures rise further or fire exposure is prolonged.

Acknowledgements

The authors have not disclosed any funding.

Data availability

The datasets generated during and/or analyzed during the current study are available from the corresponding author on reasonable request.

Conflict of interest

The authors declare that they have no conflict of interest.

References

[1] B. Behnam and H. Reza Ronagh, "A study on the effect of sequential post-earthquake fire on the performance of reinforced concrete structures," *International Journal of Structural Integrity*, Vol. 5, No. 2, pp. 141–166, May 2014, https://doi.org/10.1108/ijsi-03-2013-0005

[2] B. Behnam, H. R. Ronagh, and H. Baji, "Methodology for investigating the behavior of reinforced concrete structures subjected to post earthquake fire," *Advances in Concrete Construction*, Vol. 1, No. 1, pp. 29–44, Mar. 2013, https://doi.org/10.12989/acc.2013.1.1.029

[3] B. Behnam and H. Ronagh, "Performance of reinforced concrete structures subjected to fire following earthquake," *European Journal of Environmental and Civil Engineering*, Vol. 17, No. 4, pp. 270–292, Apr. 2013, https://doi.org/10.1080/19648189.2013.783882

[4] B. Behnam and H. Ronagh, "Performance-based vulnerability assessment of multi-story reinforced concrete structures exposed to pre – and post-earthquake fire," *Journal of Earthquake Engineering*, Vol. 18, No. 6, pp. 853–875, Aug. 2014, https://doi.org/10.1080/13632469.2014.914454

[5] E. Güvenç, "The effect of fire on the load-bearing capacity of columns," (in Turkey), Institute of Science, Niğde Ömer Halisdemir University, Niğde, Turkey, 2019.

[6] M. M. Raouffard and M. Nishiyama, "Residual load bearing capacity of reinforced concrete frames after fire," *Journal of Advanced Concrete Technology*, Vol. 14, No. 10, pp. 625–633, Oct. 2016, https://doi.org/10.3151/jact.14.625

[7] H. R. Ronagh and B. Behnam, "Investigating the effect of prior damage on the post-earthquake fire resistance of reinforced concrete portal frames," *International Journal of Concrete Structures and Materials*, Vol. 6, No. 4, pp. 209–220, Dec. 2012, https://doi.org/10.1007/s40069-012-0025-9

[8] C. Miàs, L. Torres, A. Turon, and C. Barris, "Experimental study of immediate and time-dependent deflections of GFRP reinforced concrete beams," *Composite Structures*, Vol. 96, pp. 279–285, Feb. 2013, https://doi.org/10.1016/j.compstruct.2012.08.052

[9] S. H. Alsayed, "Flexural behaviour of concrete beams reinforced with GFRP bars," *Cement and Concrete Composites*, Vol. 20, No. 1, pp. 1–11, Jan. 1998, https://doi.org/10.1016/s0958-9465(97)00061-9

[10] E. G. Nawy, G. E. Neuwerth, and C. J. Phillips, "Behavior of fiber glass reinforced concrete beams," *Journal of the Structural Division*, Vol. 97, No. 9, pp. 2203–2215, Sep. 1971, https://doi.org/10.1061/jsdeag.0002991

[11] K. V. Nakano, Y. S. Matsuzaki, H. K. Fukuyama, and M. C. Teshigawara, “Concrete beams reinforced with continuous fiber bars: flexural performance,” in *Fibre Reinforcement for Concrete Structures Symposium*, pp. 743–751, 1993.

[12] D. Kujawski, A. K. Vasudevan, and K. Sadananda, “Fatigue behavior of internal and surface cracks in vacuum,” *Engineering Fracture Mechanics*, Vol. 269, p. 108528, Jun. 2022, https://doi.org/10.1016/j.engfracmech.2022.108528

[13] R. S. Akbarova and R. S. Akbarli, “Engineering estimation of air regime of fire cut-off systems for building facades,” *Theory and Applications of Reliability*, Vol. 18, No. special issue 5, pp. 186–194, 2023.

[14] A. B. Sazairov, A. I. Z. Mehdiyev, M. R. S. Khalilov, and R. S. Akbarli, “Flexural behavior in glass fiber-reinforced beams: a finite element analysis,” *International Journal on Technical and Physical Problems of Engineering*, Vol. 16, No. 2, pp. 224–230, 2024.

[15] O. Rudenko, D. Galkina, M. Sadenova, N. Beisekenov, M. Kulisz, and M. Begentayev, “Modelling the properties of aerated concrete on the basis of raw materials and ash-and-slag wastes using machine learning paradigm,” *Frontiers in Materials*, Vol. 11, Oct. 2024, https://doi.org/10.3389/fmats.2024.1481871

[16] M. E. Issa, N. F. El-Shafey, A. T. Baraghith, and E. N. Balat, “Flexural strengthening of LWRC beams using RSHCC reinforced with glass fiber textile mesh,” *Journal of Engineering and Applied Science*, Vol. 71, No. 1, Jun. 2024, https://doi.org/10.1186/s44147-024-00467-x

[17] K. Fawzy, A. Moustafa, and M. A. Farouk, “Innovative reinforcement techniques for optimizing the performance of shallow, wide beams in reinforced concrete structures,” *Innovative Infrastructure Solutions*, Vol. 9, No. 10, Sep. 2024, https://doi.org/10.1007/s41062-024-01708-x

[18] B. A. Tayeh, B. Bayrak, A. M. Zeyad, G. Kaplan, A. Öz, and A. C. Aydın, “Effect of hybrid fibers and high temperatures on the properties of geopolymer composites based on slag, metakaolin, and natural zeolite,” *Construction and Building Materials*, Vol. 451, p. 138898, Nov. 2024, https://doi.org/10.1016/j.conbuildmat.2024.138898

[19] B. Bayrak, S. Ipek, H. G. Alcan, G. Kaplan, A. C. Aydın, and E. Güneyisi, “Engineering and microstructural properties of environmentally friendly alkali-activated composites containing clinker aggregate: heat-curing regime and elevated-temperature effect,” *Archives of Civil and Mechanical Engineering*, Vol. 24, No. 4, Jul. 2024, https://doi.org/10.1007/s43452-024-00990-x

[20] S. M. Ismoilov, M. Olimov, S. M. Abdujalilov, and D. V. Studenkova, “Elastoplastic state of a rod under three-dimensional loading considering hardening, softening, and damage susceptibility,” *Engineering Research in Russia*, Vol. 44, No. 10, pp. 1401–1405, 2024.

[21] A. Pakalniškis, G. Niaura, R. Skaudžius, A. Kareiva, and R. Ramanauskas, “Magnetic and structural transitions in multiferroic Lu(1-x)ScxFeO3 driven by temperature,” *Journal of Alloys and Compounds*, Vol. 972, p. 172805, 2024.

[22] Y. Zhang, H. Li, Q. Wang, Z. Chen, and B. Huang, “Lightweight engineered cementitious composites based on 3D-printed LC3: fresh state, hardened material characteristics, and beam performance,” *Journal of Building Engineering*, Vol. 95, p. 110085, 2024.

[23] Y. Zhang, H. Li, Q. Wang, Z. Chen, and B. Huang, “LC3-based engineered cementitious composites (LC3-ECC) with 3D printing exhibit an isotropic size effect,” *Journal of Building Engineering*, Vol. 96, p. 110215, 2024.